Experimental synchronization of circuit oscillations induced by common telegraph noise

Ken Nagai[1] and Hiroya Nakao[1,2]

[1]*Department of Physics, Graduate School of Science, Kyoto University, Kyoto 606-8502, Japan*
[2]*Abteilung Physikalische Chemie, Fritz-Haber-Institut der Max-Planck-Gesellschaft, Faradayweg 4-6, 14195 Berlin, Germany*

Experimental realization and quantitative investigation of common-noise-induced synchronization of limit-cycle oscillations subject to random telegraph signals are performed using an electronic oscillator circuit. Based on our previous formulation [K. Nagai *et al.*, Phys. Rev. E **71**, 036217 (2005)], dynamics of the circuit is described as random-phase mappings between two limit cycles. Lyapunov exponents characterizing the degree of synchronization are estimated from experimentally determined phase maps and compared with linear damping rates of phase differences measured directly. Noisy on-off intermittency of the phase difference as predicted by the theory is also confirmed experimentally.

PACS number(s): 82.40.Bj, 89.75.Da, 43.50.+y

I. INTRODUCTION

Synchronization of nonlinear dynamical elements is observed in many natural systems [1,2]. For instance, in our body, heart cells synchronize with each other to generate heartbeats, and suprachiasmatic neurons synchronize with the 24 h daily cycle to generate circadian rhythms [3,4]. Many experimental investigations of synchronization have been carried out, e.g., using coupled chemical reactors [5–7]. Synchronization typically occurs due to mutual coupling or through entrainment to common periodic signals. Generally, external noises independently applied to the elements have negative effects on synchronization; the elements cannot synchronize under independent noise sources that are too extreme.

In contrast, common or correlated external noises can synchronize uncoupled dynamical elements. Using neurons of rat neocortical slices, Mainen and Sejnowski [8] showed that reliability of spike generation improves when a neuron receives a fluctuating input current compared with the case of a constant input current. This phenomenon can be considered as synchronization of uncoupled identical dynamical elements induced by common fluctuating inputs. The synchronizing effect of common fluctuating forcing, known in ecology as the Moran effect, describes the synchronized population dynamics of organisms due to correlated environmental fluctuations [9].

More explicitly, Pikovskii [10] and Jensen [11] theoretically investigated synchronization of limit-cycle oscillators induced by nonperiodic external signals. Synchronization of uncoupled chaotic oscillators due to common noisy driving was numerically studied by Maritan and Banavar [12] and experimentally realized by Sánchez *et al.* [13] using an electronic circuit. Synchronization (or consistency) of chaotic lasers due to common fluctuating signals has also been reported [14].

For limit-cycle oscillators, general quantitative formulations of common-noise-induced synchronization can be developed using the phase-reduction method [1]. Teramae and Tanaka [15] proved that the synchronized state of uncoupled limit-cycle oscillators subject to a common weak Gaussian noise is always statistically stabilized, and their theory has been further generalized to provide global stability of phase-coherent states induced by correlated noises [16]. The cases where limit-cycle oscillators are stimulated by a common telegraph noise [17] or by a common impulsive noise [18] have also been investigated theoretically using random phase-map descriptions. Recently, synchronization due to common random impulses has been studied experimentally with an electronic circuit, and some of the theoretical predictions have been quantitatively verified [19].

In this paper, we experimentally investigate common-noise-induced synchronization using an electronic circuit undergoing periodic oscillations. As the random signal, we use a random telegraph noise, which is the simplest example of colored non-Gaussian noises. It can easily be generated in experiments and facilitates analytical treatments. In this case, we have two limit cycles corresponding to two values of the driving signal, in contrast to the previous experiment using random impulses where the system possessed only a single limit-cycle orbit [19]. When the switching interval of the driving signal is sufficiently long, the circuit state is mostly on either of the limit cycles at the moments of switching, so that its dynamics can be described in terms of phase mappings between the two limit cycles. We experimentally determine the phase maps of the electronic circuit and estimate the Lyapunov exponents characterizing the degree of synchronization from the phase maps based on our previous theory. The Lyapunov exponents are then quantitatively compared with the damping rates of small phase differences measured directly. We also confirm that noisy on-off intermittency of the phase difference, which is typically expected for random-mapping systems [17,20–23], actually occurs in our electronic circuit.

II. EXPERIMENTS

A. Setup

The experiments were performed using an electronic circuit shown schematically in Fig. 1(a), where an LM741 was used as the operational amplifier (op-amp) and the circuit parameters were set as follows: $R_1 = 100 \pm 5$ kΩ, $R_2 = 81 \pm 4.5$ kΩ, $R_3 = 470 \pm 23.5$ kΩ, $R_4 = 100 \pm 5$ Ω,
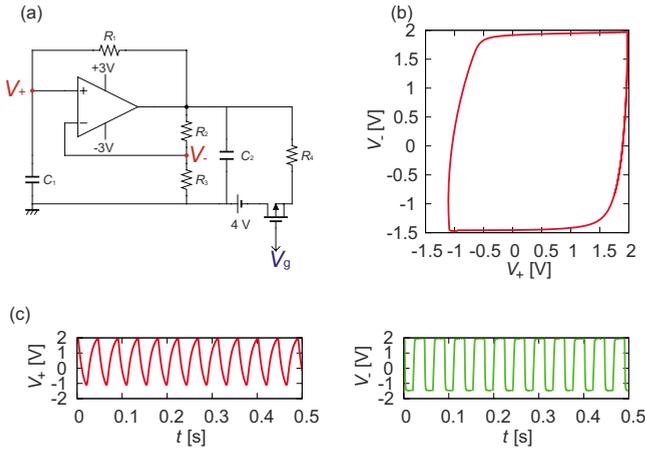
FIG. 1. (Color online) Experimental setup. (a) An electronic circuit used in the experiment. (b) A limit-cycle orbit observed at $V_g(t) \equiv -6.0$ V on the (V_+, V_-) plane. Average period was 0.0445 s. (c) Time series of $V_+(t)$ (left) and $V_-(t)$ (right).

$C_1 = 100 \pm 5$ nF, and $C_2 = 10 \pm 1$ μF. Voltages of positive and negative power supplies to the op-amp were fixed at ± 3.0 V (0 V indicates the ground voltage) using a dc power source (PMM18-2.5DU, Kikusui Electronics Co.). Note that we use the op-amp under positive feedback conditions to generate oscillations, so that the golden rule of an op-amp ($V_+ = V_-$) does not hold in our experiments.

The source voltage of the metal-oxide semiconductor field-effect transistor (MOSFET) (2SK2201, Toshiba Co.) was fixed at -4.0 V with another dc power source (E3630A, Hewlett Packard). The gate voltage $V_g(t)$ was controlled by the external signal. Voltage traces $V_+(t)$ and $V_-(t)$ were measured from the circuit as shown in Fig. 1(a). Control of $V_g(t)$ and measurements of $V_+(t)$ and $V_-(t)$ were performed with an analog-digital (AD)/digital-analog (DA) converter AIO-163202F-PE (Contec Co.). When $V_g(t)$ was fixed at a constant value between -6.0 and -2.45 V, the circuit exhibited limit-cycle oscillations. Figure 1(b) shows a limit-cycle orbit on (V_+, V_-) plane at $V_g(t) \equiv -6.0$ V, and Fig. 1(c) displays the corresponding time series of $V_+(t)$ and $V_-(t)$.

We repeatedly switched the gate voltage $V_g(t)$ between two values V_{g1} and V_{g2} to simulate a random telegraph signal. The switching events obeyed a computer-generated Poisson process, namely, the switching interval D was an exponentially distributed random variable with mean interval $\tau = 0.2$ s. We generated D by the formula $D = -1/\tau \log(1-u)$, with u being computer-generated pseudorandom numbers in [0,1]. The typical relaxation time of the circuit to converge to either of the limit cycles was shorter than 0.01 s. By applying the same time sequence of $V_g(t)$ to the circuit repeatedly, we performed consecutive measurements of the time series of $V_+(t)$, and then repeated this procedure with different realizations of the random telegraph signals. In the experiment, V_{g1} was fixed to -6.0 V and V_{g2} was varied between -6.0 and -2.45 V.

We defined a phase $\phi(t)$ of the circuit state from the time series of $V_+(t)$ as follows. The origin of the phase ($\phi = 0$) was taken as the moment when $V_+(t)$ changed its sign from negative to positive. Each time $V_+(t)$ crossed 0 V from negative to
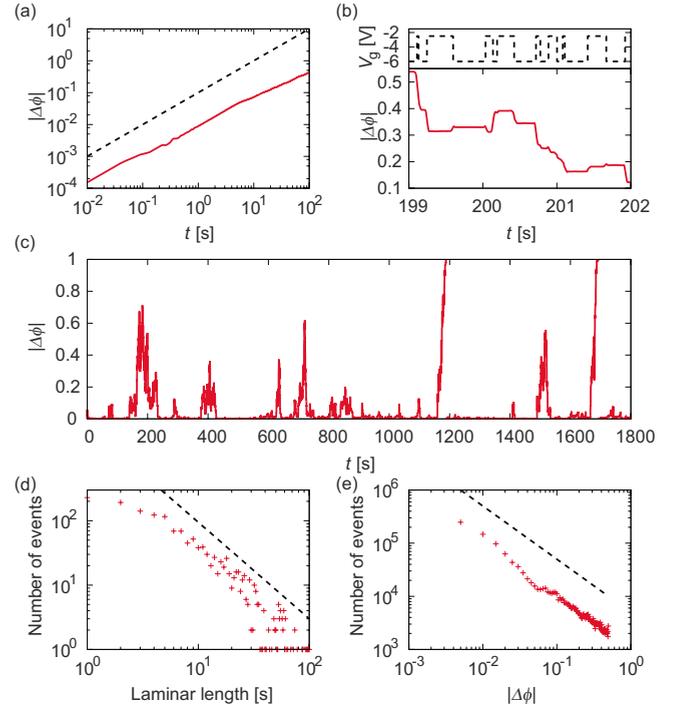

FIG. 2. (Color online) (a) Evolution of the absolute phase difference $|\Delta\phi(t)|$ under a constant external signal $V_g(t) \equiv -6.0$ V depicted using doubly logarithmic scales. The solid curve represents the experimental data and the broken line with unit slope represents linear dependence on t. [(b) and (c)] Time series of the phase difference $|\Delta\phi(t)|$ with $V_g(t)$ as a random telegraph signal ($V_{g1} = -6.0$ V and $V_{g2} = -2.5$ V): (b) short-time series of $V_g(t)$ (top) and $|\Delta\phi(t)|$ (bottom); (c) long-time series of $|\Delta\phi(t)|$, exhibiting noisy on-off intermittency. (d) Distribution of the laminar length. The broken line represents $t^{-1.5}$. (e) Distribution of the absolute phase difference $|\Delta\phi(t)|$. The broken line represents $|\Delta\phi(t)|^{-1}$.

positive, the phase was reset to 0. Between successive zero-crossing events, the phase was increased with a constant frequency from 0 to 1. Note that the frequency of the oscillator was not constant but changed from cycle to cycle due to random switching of the driving signal. From the two consecutive time series of $V_+(t)$, we obtained time series of the absolute phase differences $|\Delta\phi(t)|$ between two experimental trials (restricted to [0,1] using the periodicity of the oscillator) under the same time sequence of $V_g(t)$.

B. Results

Figure 2(a) shows the time evolution of the absolute phase difference $|\Delta\phi(t)|$ between two experimental trials under a constant input, $V_g(t) \equiv V_{g1} = -6.0$ V, which increased linearly with time t. Even after fine tuning, we observe that the average period of oscillations differed slightly across experimental trials ($\pm 0.1\%$).

Figures 2(b) and 2(c) show the time series of $\Delta\phi(t)$ observed under the common telegraph noise, where $V_g(t)$ was switched between two values ($V_{g1} = -6.0$ V and $V_{g2} = -2.5$ V). Large changes in $|\Delta\phi(t)|$ were observed only in short time windows after the switching events of $V_g(t)$ as shown in Fig. 2(b). The two experimental trials driven with

the same input signal became mostly synchronized, but occasionally there were interruptions by short desynchronization events as shown in Fig. 2(c).

To characterize this characteristic intermittent behavior of the phase difference, we measured the distribution of laminar intervals during which $|\Delta\phi(t)|$ was smaller than a certain threshold, $|\Delta\phi(t)| \leq 0.01$. As shown in Fig. 2(d), the stationary distribution of laminar intervals appeared to follow a power law, whose exponent was approximately -1.5. We also measured the stationary distribution of the absolute phase difference $|\Delta\phi(t)|$, which also exhibited a power-law tail with an exponent of roughly -1 [Fig. 2(e)]. Though the phase difference $|\Delta\phi(t)|$ shown in the figure is restricted to the range $[0,1]$, the phase difference occasionally exhibited jumps of magnitude 1 due to phase slippage of one period [e.g., near $t=1200$ and $t=1600$ in Fig. 2(c)] [24].

Thus, when the gate voltage $V_g(t)$ was switched between two values randomly, different experimental trials tended to be synchronized even under the effect of slight differences in average periods and experimental noise. As we explain later, the characteristic behavior of the phase difference $|\Delta\phi(t)|$ was due to noisy on-off intermittency [17,20–23].

III. ANALYSIS

A. Theory

Here we briefly summarize our previous theory on the synchronization of uncoupled oscillators driven by a common random telegraph signal [17]. Corresponding to the two different values of the input signal $V_g(t)$, the circuit exhibits two different limit cycles, LC1 for $V_g(t) \equiv V_{g1}$ and LC2 for $V_g(t) \equiv V_{g2}$. When $V_g(t) \equiv V_{g1}$, we can define a phase $0 \leq \theta_1(V_+, V_-) < 1$ for LC1 and also in the (V_+, V_-) plane, which increases with a constant frequency $1/T_1$, with T_1 as the period of LC1 [1,3]. Similarly, when $V_g(t) \equiv V_{g2}$, another phase $0 \leq \theta_2(V_+, V_-) < 1$ can be defined in the (V_+, V_-) plane that increases with a constant frequency $1/T_2$, where T_2 is the period of LC2. The origins of θ_1 and θ_2 are taken as the points where $V_+(t)$ crosses 0 V from negative to positive on LC1 or LC2. Combining these, we introduce a new phase $\theta(V_+, V_-, V_g)$ of the circuit state as

$$\theta(V_+, V_-, V_g) = \begin{cases} \theta_1(V_+, V_-) & \text{when } V_g = V_{g1} \\ \theta_2(V_+, V_-) & \text{when } V_g = V_{g2} \end{cases} \quad (1)$$

Note that this θ is different from the phase ϕ that we defined in Sec. II by linearly interpolating successive zero-crossing events. θ jumps discontinuously at the moments when $V_g(t)$ switches, because θ_1 and θ_2 increase with strictly constant frequencies. In contrast, ϕ is continuous even when $V_g(t)$ is fluctuating [except the zero-crossing events of $V_+(t)$], but its frequency differs from cycle to cycle. When $V_g(t)$ is kept constant for longer than one period of oscillation and than the relaxation time of the circuit to the limit cycle, ϕ coincides with θ. This difference in the definition of the phase variables yields only small bounded discrepancies in measuring the phase differences between two time series.

We assume that the average switching time of the input signal, τ, is sufficiently longer than the relaxation time of the
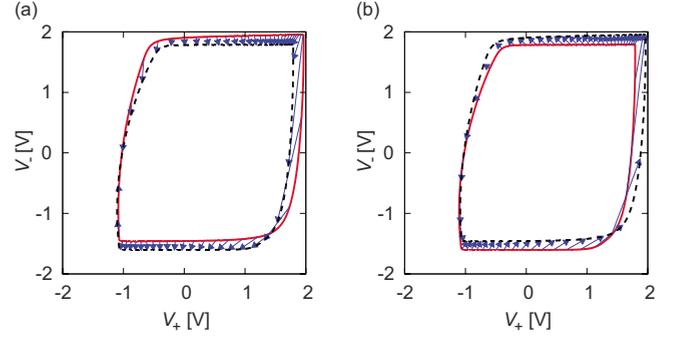

FIG. 3. (Color online) Phase mappings between two limit cycles. (a) When $V_g(t)$ switches from $V_{g1}=-6.0$ V to $V_{g2}=-2.45$ V, points on LC1 (solid curve) for V_{g1} are mapped to the corresponding points on LC2 (broken curve) for V_{g2} as indicated by arrows. (b) From $V_{g2}=-2.45$ V to $V_{g1}=-6.0$ V.

orbit to LC1 or LC2 at fixed $V_g(t)$. In our experiments, we took $\tau=0.2$ s and the relaxation time was typically shorter than 0.01 s, so that this condition was satisfied. The orbit of the circuit is then almost always on one of the limit cycles when $V_g(t)$ is switched between two values. Therefore, we can describe the dynamics of the circuit under randomly switched $V_g(t)$ as alternating phase mappings between θ_1 and θ_2 as shown in Fig. 3. We denote the mapping from θ_1 to θ_2 that takes place when $V_g(t)$ switches from V_{g1} to V_{g2} as $\theta_2 = f_{12}(\theta_1)$, and the mapping from θ_2 to θ_1 when $V_g(t)$ switches from V_{g2} to V_{g1} as $\theta_1 = f_{21}(\theta_2)$ [17].

Let us denote the phase on LC1 just before $V_g(t)$ switches from V_{g1} to V_{g2} for the nth time as θ_1^n, and the phase on LC2 just before $V_g(t)$ switches from V_{g2} to V_{g1} for the nth time as θ_2^n. Then the phase dynamics of the orbit can be described as [assuming $V_g(t=0)=V_{g1}$]

$$\theta_1^{n+1} = f_{21}(\theta_2^n) + s_1^{n+1}, \quad \theta_2^n = f_{12}(\theta_1^n) + s_2^n, \quad (2)$$

where s_1^n and s_2^n are exponentially distributed random switching intervals whose probability distributions are given by

$$P_1(s_1^n) = \frac{T_1}{\tau}\exp\left(-\frac{s_1^n T_1}{\tau}\right), \quad P_2(s_2^n) = \frac{T_2}{\tau}\exp\left(-\frac{s_2^n T_2}{\tau}\right), \quad (3)$$

respectively. Small deviations $\Delta\theta_1^n$, $\Delta\theta_2^n$ from θ_1^n, θ_2^n obey linearized equations

$$\Delta\theta_1^{n+1} = f_{21}'(\theta_2^n)\Delta\theta_2^n, \quad \Delta\theta_2^n = f_{12}'(\theta_1^n)\Delta\theta_1^n, \quad (4)$$

where f' denotes the derivative function of f. After the nth switching, the amplitude of the deviation $\Delta\theta_1^n$ is given by

$$|\Delta\theta_1^n| = \left(\prod_{i=1}^{n-1} |f_{12}'(\theta_1^i)||f_{21}'(\theta_2^i)|\right)|\Delta\theta_1^1|, \quad (5)$$

and $|\Delta\theta_2^n|$ similarly. Thus, for large n,

$$\frac{|\Delta\theta_1^n|}{|\Delta\theta_1^1|} = \frac{|\Delta\theta_2^n|}{|\Delta\theta_2^1|} \simeq \exp(\lambda n) \quad (6)$$

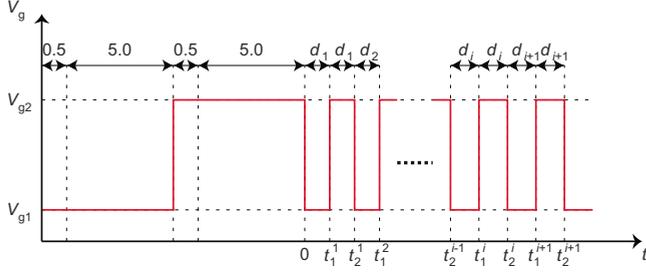holds, where the Lyapunov exponent λ is given by

FIG. 4. (Color online) The probe signal used to determine the phase maps. Before $t=0$, T_1 and T_2 were measured. After $t=0$, the phases were measured at t_1^i and t_2^i for $1 \le i \le 200$.

$$\lambda = \lim_{n \to \infty} \frac{1}{n} \ln\left(\prod_{i=1}^{n} |f_{12}'(\theta_1^i)||f_{21}'(\theta_2^i)| \right) = \lambda_1 + \lambda_2, \quad (7)$$

with

$$\lambda_1 \simeq \int_0^1 d\theta_1 \ln|f_{12}'(\theta_1)|, \quad \lambda_2 \simeq \int_0^1 d\theta_2 \ln|f_{21}'(\theta_2)|. \quad (8)$$

Here, we approximate the average over the stationary distribution of the phase θ_1 or θ_2 under the effect of telegraph noises by the average over the uniform distribution in each equation, because the phases θ_1 and θ_2 are almost uniformly distributed on LC1 and LC2 when τ is sufficiently larger than T_1 and T_2 [17]. In our experiments, we used $\tau=0.2$, whereas the period of oscillations was about 0.05 s. Therefore, this condition was satisfied.

When $\lambda=\lambda_1+\lambda_2<0$, phase synchronization induced by the random telegraph signal is expected. Note that the switching step n is approximately related to the real time t as $n \simeq t/2\tau$, so that

$$\frac{|\Delta\theta(t)|}{|\Delta\theta(0)|} \simeq \exp\left(\frac{\lambda}{2\tau} t \right) \quad (9)$$

holds for large n, t.

B. Determination of phase maps

We experimentally determined the phase maps $\theta_1 = f_{21}(\theta_2)$ and $\theta_2 = f_{12}(\theta_1)$ as follows. We first measured the period T_1 of LC1 under a constant input signal $V_g(t) \equiv V_{g1}$. After setting $V_g(t)$ at V_{g1} and relaxing the circuit for 0.5 s, intervals between successive zero-crossing events of $V_+(t)$ from negative to positive values were measured for 5 s. T_1 was determined by averaging these intervals. We then measured the period T_2 of LC2 at $V_g(t) \equiv V_{g2}$ in a similar way.

When the measurement of T_2 was completed (this moment was defined as $t=0$), the following *regular* telegraph signal (shown schematically in Fig. 4) was applied as the probing input:

$$V_g(t) = \begin{cases} V_{g1}, & t_2^{i-1} \le t < t_1^i \\ V_{g2}, & t_1^i \le t < t_2^i, \end{cases} \quad (10)$$

for $i=1,\dots,200$, where the ith switching time from V_{g1} to V_{g2} is given by

$$t_1^1 = d_1, \quad t_1^i = d_i + \sum_{k=1}^{i-1} 2d_k, \quad i \ge 2, \quad (11)$$

and the subsequent ith switching time from V_{g2} to V_{g1} is given by

$$t_2^i = \sum_{k=1}^{i} 2d_k, \quad i \ge 1. \quad (12)$$

Here, d_i denotes the length of the ith constant interval of the input signal. To avoid undesirable synchronization with the probe signal, we gradually increased d_i as $d_i=0.5+0.001(i-1)$ ($1 \le i \le 200$).

Using this $V_g(t)$, we measured the phase $0 \le \Phi_1^i < 1$ of the circuit at t_1^i,

$$\{(\Phi_1^i, t_1^i)|i=1,\dots,200\}, \quad (13)$$

and the phase $0 \le \Phi_2^i < 1$ of the circuit at t_2^i,

$$\{(\Phi_2^i, t_2^i)|i=1,\dots,200\}. \quad (14)$$

These phases Φ_1^i and Φ_2^i can be identified with the phases θ_1 and θ_2 used in the theory via

$$\theta_1(t=t_1^i) = \Phi_1^i, \quad \theta_2(t=t_2^i) = \Phi_2^i. \quad (15)$$

Note that the two types of the phases coincide here because the constant intervals d_i of the probe signal are always longer than T_1, T_2, and the relaxation time of the circuit to LC1 or LC2.

At each switching event, the phase jumped from Φ_1^i to $\tilde{\Phi}_2^i$ ($V_{g1} \to V_{g2}$), or from Φ_2^i to $\tilde{\Phi}_1^i$ ($V_{g2} \to V_{g1}$). The destination phases $\tilde{\Phi}_1^i$ and $\tilde{\Phi}_2^i$ just after t_1^i and t_2^i were obtained from Φ_1^i and Φ_2^i as

$$\tilde{\Phi}_1^i = \left(\Phi_1^{i+1} - \frac{d_{i+1}}{T_1} \right) \bmod 1, \quad \tilde{\Phi}_2^i = \left(\Phi_2^i - \frac{d_i}{T_2} \right) \bmod 1, \quad (16)$$

where the definitions were made modulo 1 to restrict the phases to [0,1]. Thus, we obtained 200 realizations of the phase mappings,

$$\{\Phi_2^i \to \tilde{\Phi}_1^i|i=1,\dots,200\}, \quad \{\Phi_1^i \to \tilde{\Phi}_2^i|i=1,\dots,200\}. \quad (17)$$

We constructed the raw phase maps by piecewise linearly interpolating these data as

$$\tilde{\Phi}_2 = f_{12}^{\mathrm{raw}}(\Phi_1), \quad \tilde{\Phi}_1 = f_{21}^{\mathrm{raw}}(\Phi_2), \quad (18)$$

which were still nonsmooth functions due to experimental fluctuations.

Generally, the phase map has a trivial diagonal component, namely, the identity-map component that exists even when $V_{g1}=V_{g2}$, and additional nontrivial components reflecting the nonlinear transition dynamics between the limit cycles. We estimated the underlying smooth phase maps f_{12} and f_{21} from the raw phase maps f_{12}^{raw} and f_{21}^{raw} by low-pass filtering using the 20 lowest Fourier modes as

$$f_{12}(\theta_1) = \theta_1 + \sum_{k=-20}^{20} c_{12}^k \exp(2\pi k i \theta_1),$$

$$f_{21}(\theta_2) = \theta_2 + \sum_{k=-20}^{20} c_{21}^k \exp(2\pi k i \theta_2), \quad (19)$$

where c_{12}^k and c_{21}^k are Fourier coefficients of the nontrivial components of f_{12}^{raw} and f_{21}^{raw}, defined as

$$f_{12}^{\text{raw}}(\Phi_1) - \Phi_1 = \sum_{k=-\infty}^{\infty} c_{12}^k \exp(2\pi k i \Phi_1),$$

$$f_{21}^{\text{raw}}(\Phi_2) - \Phi_2 = \sum_{k=-\infty}^{\infty} c_{21}^k \exp(2\pi k i \Phi_2). \quad (20)$$

Figure 5(a) displays examples of the phase maps obtained with the above procedure.

C. Lyapunov exponents and damping rates

From the experimentally determined phase maps $f_{12}(\theta_1)$ and $f_{21}(\theta_2)$, the Lyapunov exponent $\lambda = \lambda_1 + \lambda_2$ can be estimated. This λ can be compared with the damping rate r_{damp} of small phase differences between two trials subject to the same telegraph noise. As we have already explained, the difference in the definitions of two phases results in only a small bounded discrepancy between $\Delta\theta(t)$ and $\Delta\phi(t)$, so that it does not affect the Lyapunov exponents or the damping rates.

When the phase difference $\Delta\phi(t)$ is small, we expect the ensemble average of $\Delta\phi(t)$ over many realizations of the random telegraph signal to shrink exponentially as

$$\langle|\Delta\phi(t)|\rangle \sim \exp(r_{\text{damp}}t), \quad (21)$$

where $r_{\text{damp}} < 0$ is the damping rate. As the average switching interval of $V_g(t)$ is τ,

$$r_{\text{damp}} = \frac{\lambda}{2\tau} \quad (22)$$

will approximately hold for large t and n provided that the previous analysis based on the phase-mapping description is reasonable.

Figure 5(b) compares the Lyapunov exponent λ with the damping rate r_{damp} obtained for different values of V_{g2} with fixed V_{g1}. The damping rate r_{damp} was directly measured from $|\Delta\phi(t)|$ as

$$r_{\text{damp}} = \frac{1}{M^{-1}\sum_{k=1}^{M}\Delta T_k}\ln\left|\frac{\Delta\phi_{\text{lower}}}{\Delta\phi_{\text{upper}}}\right|, \quad (23)$$

where $\Delta\phi_{\text{upper}} = 0.2$, $\Delta\phi_{\text{lower}} = 0.05$, ΔT_k is the time needed for $|\Delta\phi|$ to be damped from $\Delta\phi_{\text{upper}}$ to $\Delta\phi_{\text{lower}}$, and M is the number of such shrinkage events in the time series of $|\Delta\phi(t)|$. We measured 20 time sequences of $V_+(t)$ for 120 s and calculated 19 time sequences of the phase difference $\Delta\phi(t)$ between two consecutive time sequences of $V_+(t)$ to obtain r_{damp}. As shown in Fig. 5(c), pairs of $(\lambda, r_{\text{damp}})$ esti-
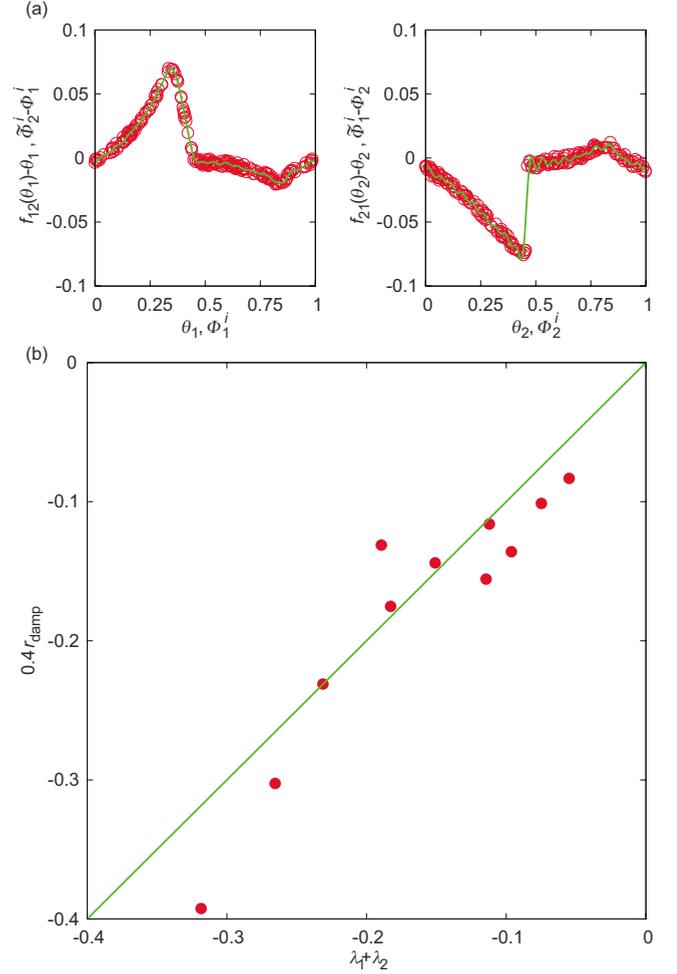

FIG. 5. (Color online) (a) Experimentally determined phase maps. Circles show the raw data $(\Phi_1^i, \tilde{\Phi}_2^i - \Phi_1^i)$ (left) or $(\Phi_2^i, \tilde{\Phi}_1^i - \Phi_2^i)$ (right), and curves represent the nontrivial part of the estimated phase maps $f_{12}(\theta_1) - \theta_1$ (left) or $f_{21}(\theta_2) - \theta_2$ (right) obtained after low-pass filtering. $V_{g1} = -6.0$ V and $V_{g2} = -2.5$ V. (b) Comparison of the Lyapunov exponents $\lambda = \lambda_1 + \lambda_2$ with the linear damping rates r_{damp} directly measured from $|\Delta\phi(t)|$. The line represents $0.4 r_{\text{damp}} = \lambda_1 + \lambda_2$. Filled circles represent the data obtained by varying V_{g2} (-2.55 V $\leq V_{g2} \leq -2.45$ V with intervals of 0.01 V) while fixing V_{g1} at -6.0 V.

mated for various values of V_{g2} approximately fall on the straight line $\lambda = 0.4 \, r_{\text{damp}}$ ($\tau = 0.2$ in the experiment), which quantitatively verifies the validity of the phase-mapping description of our experiments.

D. Noisy on-off intermittency

We have focused so far on the average behavior of the phase difference. The phase difference $|\Delta\phi(t)|$ decreases on average when $\lambda = \lambda_1 + \lambda_2 < 0$. However, as can be seen from Eq. (5), small phase differences $\Delta\theta_1$ and $\Delta\theta_2$ are driven multiplicatively by the random application of two phase maps. This is a typical situation where noisy on-off (or modulational) intermittency is expected over long time scales [17,20–23]. Due to small noises or heterogeneity inherent in the system, individual time sequence of $|\Delta\phi(t)|$ can occa-

sionally grow due to random multiplication even if $\lambda = \lambda_1 + \lambda_2 < 0$, resulting in repetitive transient bursting. As already shown in Figs. 2(d) and 2(e), this is the case for our electronic circuit. The power-law distribution of the laminar interval with the exponent of -1.5 as shown in Fig. 2(d), and the power-law distribution of the amplitude of the phase difference as shown in Fig. 2(e) are consistent with the theoretical predictions on noisy on-off intermittency [20–23].

IV. CONCLUSIONS

We investigated synchronization between different experimental trials induced by common telegraph noises using an electronic circuit undergoing limit-cycle oscillations. The dynamics of the circuit could be described in terms of random-phase mappings. We experimentally determined the phase maps and quantitatively verified that the Lyapunov exponents determined from the phase maps agreed with the damping rates measured directly from the time series of small phase differences. We also confirmed that noisy on-off intermittency of the phase difference actually occurs.

The mechanism leading to synchronization that we demonstrated using an electronic circuit in this paper is general and is expected to be observed in various systems undergoing limit-cycle oscillations.

[1] Y. Kuramoto, *Chemical Oscillations, Waves, and Turbulence* (Springer-Verlag, Berlin, 1984).

[2] S. H. Strogatz, *Nonlinear Dynamics and Chaos: With Applications to Physics, Biology, Chemistry and Engineering* (Perseus, Cambridge, MA, 1994).

[3] A. T. Winfree, *The Geometry of Biological Time* (Springer-Verlag, New York, 2001).

[4] B. Rusak and I. Zucker, Physiol. Rev. **59**, 449 (1979).

[5] M. Marek and I. Stuchl, Biophys. Chem. **3**, 241 (1975).

[6] M. Yoshimoto, K. Yoshikawa, and Y. Mori, Phys. Rev. E **47**, 864 (1993).

[7] H. Fukuda, H. Morimura, and S. Kai, Physica D **205**, 80 (2005).

[8] Z. F. Mainen and T. J. Sejnowski, Science **268**, 1503 (1995).

[9] B. T. Grenfell, K. Wilson, B. F. Finkenstädt, T. N. Coulson, S. Murray, S. D. Albon, J. M. Pemberton, T. H. Clutton-Brock, and M. J. Crawley, Nature (London) **394**, 674 (1998).

[10] A. S. Pikovskii, Radiophys. Quantum Electron. **27**, 390 (1984).

[11] R. V. Jensen, Am. J. Phys. **70**, 607 (2002).

[12] A. Maritan and J. R. Banavar, Phys. Rev. Lett. **72**, 1451 (1994).

[13] E. Sánchez, M. A. Matías, and V. Pérez-Muñuzuri, Phys. Rev. E **56**, 4068 (1997).

[14] A. Uchida, R. McAllister, and R. Roy, Phys. Rev. Lett. **93**, 244102 (2004).

[15] J. N. Teramae and D. Tanaka, Phys. Rev. Lett. **93**, 204103 (2004).

[16] H. Nakao, K. Arai, and Y. Kawamura, Phys. Rev. Lett. **98**, 184101 (2007).

[17] K. Nagai, H. Nakao, and Y. Tsubo, Phys. Rev. E **71**, 036217 (2005).

[18] H. Nakao, K. S. Arai, K. Nagai, Y. Tsubo, and Y. Kuramoto, Phys. Rev. E **72**, 026220 (2005).

[19] K. Arai and H. Nakao, Phys. Rev. E **77**, 036218 (2008).

[20] H. Fujisaka and T. Yamada, Prog. Theor. Phys. **74**, 918 (1985).

[21] A. Čenys, A. N. Anagnostopoulos, and G. L. Bleris, Phys. Lett. A **224**, 346 (1997).

[22] A. S. Pikovsky, Phys. Lett. A **165**, 33 (1992).

[23] H. Nakao, Phys. Rev. E **58**, 1591 (1998).

[24] K. Yoshimura, P. Davis, and A. Uchida, Prog. Theor. Phys. **120**, 621 (2008).